IEEE Access
Multidisciplinary | Rapid Review | Open Access Journal

Received December 3, 2019, accepted December 29, 2019, date of publication January 8, 2020, date of current version January 17, 2020.

Digital Object Identifier 10.1109/ACCESS.2020.2965082

Cuff-Less Blood Pressure Monitoring System Using Smartphones

FATEMEHSADAT TABEI[1], JON MICHAEL GRESHAM[1], BEHNAM ASKARIAN[1], KWANGHEE JUNG[2], AND JO WOON CHONG[1]

[1]Department of Electrical and Computer Engineering, Texas Tech University, Lubbock, TX 79409-3102, USA
[2]Department of Educational Psychology and Leadership, Texas Tech University, Lubbock, TX 79409-1071, USA

Corresponding authors: Kwanghee Jung (kwanghee.jung@ttu.edu) and Jo Woon Chong (j.chong@ttu.edu)

This work was supported by the National Heart, Lung, and Blood Institute of the National Institutes of Health under award number R15 HL121761.

ABSTRACT Recently, smartphones with mobile health applications have become promising tools in the healthcare industry due to their convenience, ubiquity for patients, and the ability to gather data in real time. In this paper, we propose a novel non-invasive, portable, and cuff-less method for monitoring BP by only using the smartphones' camera. Our experiment uses pulse transit time (PTT) between two separate photoplethysmogram (PPG) signals to estimate the subjects' systolic blood pressure (SBP) and diastolic blood pressure (DBP). Our proposed method first measures the subject's PPG signals from his/her index fingers using the smartphones' camera. Then, filtering and peak detection algorithms of the proposed method reduce the motion and noise artifacts in the PPG signals. Finally, the proposed method estimates SBP and DBP based on a linear regression model which was trained and tested on 30 trials with six healthy subjects. We evaluated the proposed method by comparing BP values of the proposed method with those of the reference (or gold-standard) device in terms of mean absolute error (*MAE*), standard deviation of error (*SD*), and R-squared (R^2) value of the cross-validation. Experimental results show that the proposed method estimates the average of $MAE \pm SD$ is 2.07 ± 2.06 mm Hg for SBP estimation, and 2.12 ± 1.85 mm Hg for DBP estimation. These estimates are lower than accurate BP estimation standard (5 ± 8 mmHg).

INDEX TERMS Hypertension, blood pressure, cuff-less, smartphone, photoplethysmogram (PPG), pulse transit time (PTT).

I. INTRODUCTION

Hypertension (or high blood pressure [BP]) is a significant health issue for adults that can result in serious complications, such as stroke and heart diseases [1]. It is estimated that 1.3 billion people worldwide are currently affected by high BP [2]. Specifically, one out of three adults in the U.S. suffer from hypertension, according to a report from the Centers for Disease Control and Prevention, but less than half of those (46%) have been controlling their BP [1]. A report from the *Journal of the American Heart Association* shows that the annual healthcare cost for an individual with hypertension is more than $2,000 [3]. Hence, continuous BP monitoring of patients suffering from hypertension can prevent the progression of the hypertension and reduce medical costs.

There have been invasive and non-invasive BP measurement methods. Catheterization is the most exact method. It involves placing a strain gauge in fluid contact with a patient's blood at any of their arterial sites, which allows instantaneous measurement of the patient's BP [4]. However, this method is invasive, often painful or uncomfortable for patients to use, and cannot be used for outpatient monitoring. Another method, the mercury sphygmomanometer, is a non-invasive BP measurement method that uses an inflatable cuff [5]. Oscillometry is another conventional and non-invasive method that requires a cuff [6], [7]. Tonometry is a clinical method for continuous BP monitoring, which obtain the arterial waveform using sensors located on the artery sites [8]–[10]. Volume clamping uses a photoplethysmogram (PPG) signal and an inflatable cuff to measure the BP [11]. Some drawbacks of these methods are that the equipment is cumbersome to carry, time-consuming to use, and inconvenient for portability [4], [12]–[14].

Progress has also been made in cuff-less BP monitoring to overcome the portability issue. The pulse wave analysis (PWA), pulse arrival time (PAT), and pulse transit

The associate editor coordinating the review of this manuscript and approving it for publication was Venkata Rajesh Pamula.

time (PTT) [15]–[24] are typicall adopted in cuff-less BP measurement studies. The PWA methods use the pulse pressure, or pulse wave velocity (PWV), to perform BP estimation [15], [16]. The PWV is the velocity of propagation of the pressure waves that occur across the line of the arteries as blood pumps through the individual's circulatory system [4]. A wearable BP measurement device based on PWV analysis was proposed in [25]. The PWV parameter was calculated by using PPG signals from two different arterial parts. One PPG signal was derived from a sensor attached to the ulna arterial site, and the other PPG signal was derived from a sensor attached to the digital artery with a known distance from the first PPG sensor. When deriving PWV, other parameters, such as the dimension of the vessel, the elasticity of the arterial wall, and blood density, are often required [16], [21]. The pulse pressure can be obtained by ultrasound to estimate the arterial BP [20]. However, this method can be used only in clinical applications, since it requires clinicians/technical staff to work with an ultrasound probe. PAT is the amount of time it takes for the pulse to arrive from the heart to an arterial site, and can be used in research in combination with PTT [24]. It has been shown that PAT is not a significant enough indicator to estimate BP compared to PTT. Hence, PTT is the main methodology adopted in cuff-less BP monitoring.

Previous cuff-less and PTT-based studies are typically classified into three categories [4], [10]: 1) adopting only an electrocardiogram (ECG) signal [26], [27], 2) adopting both ECG and PPG signals [28]–[32], and 3) adopting only a PPG signal [22], [23], [33]. The research adopting the approaches of *1)* and *2)* can be difficult to apply in daily life, since the ECG signal is derived from sensors attached to the body. On the other hand, the PTT-based research which requires the detection of the PPG signals adopting the approach of *3)* is more desirable for daily applications. This is because the PPG signals can be acquired by simply placing a sensor on the subject's fingertip. Wearable BP monitoring devices which use PPG signals and PTT algorithms have been proposed [34]–[37]. Specifically, three sensors were embedded on a wearable glass to measure the PPG from three different locations on the face (angular artery, superficial temporal, and occipital artery) to derive the PTT and estimate the BP [37]. Two PPG signals acquired from a smartwatch (CareUp) were used to estimate the blood pressure [38]. The PTT was derived from the time difference between the PPG of the fingertip of one hand and the PPG of the wrist of the opposite hand [38]. Then the blood pressure was linearly modeled to the PTT and heart rate variability. This model was chosen because it had the least computational complexity that could be handled in a wearable smartwatch with low random-access memory (RAM) capacity. These wearable BP monitoring methods often require additional sensors to acquire PPG signals for BP estimation.

Smartphones have emerged in healthcare monitoring applications due to their ease of use and availability. Recent studies have also detected PPG signals from a smartphone. These smartphone methods can be used for heart rate estimation, atrial fibrillation detection, oxygen saturation measurement, and BP estimation [39]–[45]. Two smartphones were used in [42] to record the audio signal and the PPG signal together to estimate BP. The PTT was calculated from the heartbeat sound acquired from one smartphone and the PPG signal acquired from a fingertip using another smartphone. The iCare health monitor [46] provided a smartphone application for BP estimation. The application used the PPG signal from the camera and finger pressure on the touch screen sensor [47]. The Seismo [48] proposed a method to monitor BP using the smartphone's accelerometer and camera. The PTT was calculated as the time between the blood ejection from the heart and the pulse reaching the fingertip. The blood ejection time was captured from the seismocardiography signal using the smartphone's accelerometer, and the arrival time at the fingertip was measured with the PPG using the smartphone's camera. In [45] one smartphone was used to acquire the PTT from the fingertip and forehead PPG signals. However, to the authors' knowledge, there is not any research available that captures the PTT from two fingertip sites using only PPG signals.

In this paper, we propose a cuff-less BP monitoring system that estimates BP with high accuracy and reliability. Our algorithm uses PTT obtained from smartphone PPG signals to estimate BP. Specifically, we use two identical iPhones for PPG measurement and PTT calculation to overcome the frame rate and different specifications. Our system also provides easier access by using only smartphones, without any use of additional devices or sensors. We trained our linear regression using a leave-one-out cross-validation algorithm to derive the individual-specific parameter of the BP estimation model. The acquired individual-specific parameters were then tested on the remaining trials to estimate the systolic blood pressure (SBP) and diastolic blood pressure (DBP) values. The results of our proposed cuff-less BP estimation model were evaluated using statistical parameters such as mean absolute error (*MAE*), standard deviation of error (*SD*), and root-mean-square error (*RMSE*). We also evaluate the predicted BP values in terms of the correlation coefficient for all the subjects and both SBP and DBP estimations. The rest of this paper consists as follows: Section II describes the data acquisition and materials of the study. The preprocessing steps for PTT calculation along with the linear regression model for BP estimation are explained in Section III. Section IV presents the results of our study performed on six healthy subjects with 30 trials per subject, and, finally, Section V concludes the paper.

II. MATERIALS

For this paper, we used two identical smartphone models (iPhone X [49]) simultaneously in the experiment to measure and estimate BP from the subjects to derive the PPG signals. The sampling rate of both smartphones' cameras is 30 frames per second (fps). Specifically, we adopted identical smartphones to exclude any possible difference in technical

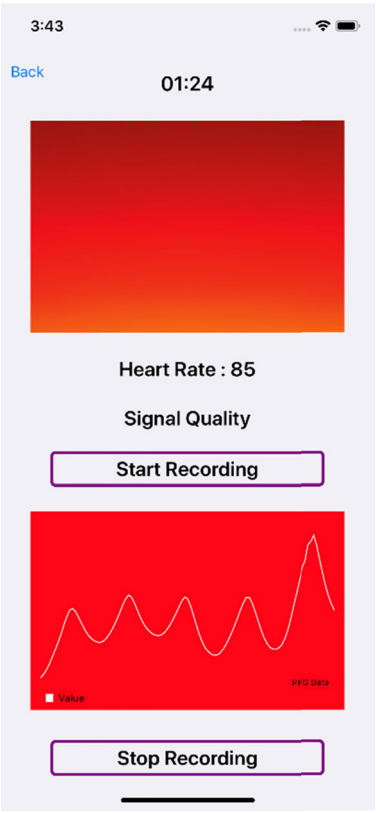

FIGURE 1. Screenshot of the developed iOS application for extracting PPG signals. The red rectangular box on the top of the screen shows the captured RGB frame from the smartphone's camera video recording. The real-time PPG signal is shown in the bottom red box, and the timer shows the remaining time of the measurement.

specifications of the smartphones' cameras, such as different sampling rates, which could affect the PTT measurement.

Fig. 1 shows the screenshot of the proposed application. The red rectangular box on top is the captured frame from the smartphone video recording, and the measured PPG signal is shown in the bottom box of the app's screen in real time. Furthermore, the app shows the remaining time of the total duration of the measurement, which was used to assure that the start time and end time of the measurements were synchronized. Our proposed developed iOS application, which was installed on both phones, was used to extract the PPG signals. The PPG signals were measured from the index fingers of a subject after the fingers were placed over the smartphones' camera sensors. The installed application processed the RGB frames of the smartphone video recording, and the average intensity values of the green channel were used to derive the PPG signals.

For this study, six subjects who did not have hypertension were recruited following Texas Tech University's Institutional Review Board (IRB# 2018-742) protocol. The subjects were asked to sit relaxed in a chair. They were asked to minimize any movement since it could cause motion and noise artifacts (MNA) in the smartphone PPG recordings. The digital cuff-based OMRON 10 series [50] BP monitor device (as shown in Fig. 2a) was used as the gold standard

(a)

(b)

FIGURE 2. Experimental setup of the data acquisition. (a) The actual BP measurement using a digital BP monitoring device (OMRON 10 series), and (b) the subjects were asked to place the index finger of their right and left hand on the iPhone X's rear camera sensors to acquire the PPG signal using the developed iOS application.

method to get the actual BP values. These values were later compared with the subject's estimated BP. For the actual BP measurement, the subject's left bicep was wrapped with the inflatable cuff while the subject's arm was positioned on a desk in a relaxed position. The actual BP values of each subject were then documented in a spreadsheet. Next, the PPG signals from the subjects were gathered using the two smartphones simultaneously. The actual BP measurement with the OMRON device used as a reference was done before starting each data trial from the two smartphones.

The recorded PPG signals from the smartphones were then transferred to a computer for further analysis. It is important to note that the actual BP measurement and the estimated BP derived from the video recordings of the two smartphones were not performed simultaneously since the

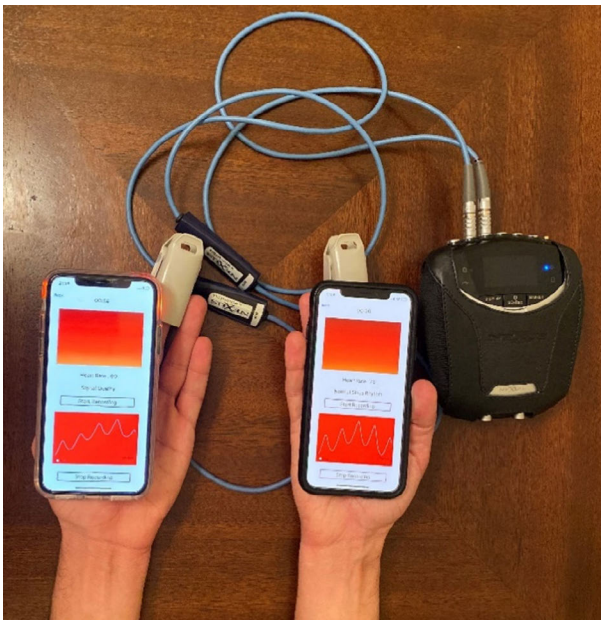

FIGURE 3. Data acquisition setup of the evaluation procedure to compare the smartphones' sampling frequency with the reference PPG device. The NeXus-10 MK II was used simultaneously with the smartphones to compare the PTT values. The subjects were asked to place the index fingers of their right and left hands on the iPhone X's rear camera sensors to acquire the PPG signals using the developed iOS application. The NeXus PPG sensors were attached to the middle fingers of the test subject to acquire reference PPG signals.

cuff pressure could affect the recordings of the PPG signals from the subject's index fingers during the data trials. The time gap between the actual BP measurement and the smartphone measurement was less than 1 minute. Fig. 2 shows the experimental settings of the actual BP measurement and the procedure of the smartphones' data acquisition.

For each data trial, the smartphone recording lasted 120 seconds, and a series of 30 separate data trials were performed on each test subject. The trials from each subject were taken at different times of the day between 10 am and 4 pm. Specifically, each subject was asked to participate in the data acquisition procedure in two phases. One set of measurements was acquired in the morning and the other set of measurements was done in the afternoon. Moreover, after 5 trials per subject, the data acquisition procedure was paused, and the subjects were asked to stand up and walk around for 5 minutes. The data acquisition protocol was set to have a slight variation of BP during normal and easy daily activities.

As mentioned above, the sampling rate of the smartphone's camera was limited to 30 fps. Therefore, we evaluated the performance of PTT estimation of our proposed method by comparing the PTT estimation of the proposed method to that of the reference method. Here, we used NeXus-10 MK II [51] as a reference. The comparison was performed on one test subject by 1) measuring the actual BP, and 2) measuring the smartphone PPG signals from the left and right hands while the PPG signals from both hands using the NeXus device were also measured simultaneously. The sampling frequency of the NeXus device was set as 256 Hz, and 30 trials of the evaluation procedure were measured from a test subject. Fig. 3 shows the data acquisition setting for the evaluation procedure. A test subject was asked to place the index fingers of both left and right hands on the rear cameras of the smartphones while the PPG sensors of the NeXus device were attached to the middle fingers of both hands as shown in Fig. 3. The actual BP measurement procedure was performed by the OMRON device as shown in Fig. 2a.

III. METHODS

Fig. 4 shows a flowchart of the preprocessing and the proposed BP estimation method. After the data acquisition, the signals were preprocessed for further analysis of BP estimation, using a mathematical model of the BP and PTT relationship to derive the estimated values of the subject's BP. The preprocessing step is explained in detail in Subsection III-A. Subsection III-B explains the relationship between the BP and the PTT, and the mathematical model used to derive the subject's estimated BP values.

A. PREPROCESSING

The acquired PPG signals from the smartphones using the developed application were first passed through a high-pass filter with a cutoff frequency of 0.5Hz. The baseline in the PPG signals was removed in this step. To filter out unwanted peaks and create a smooth signal, a moving average filter with

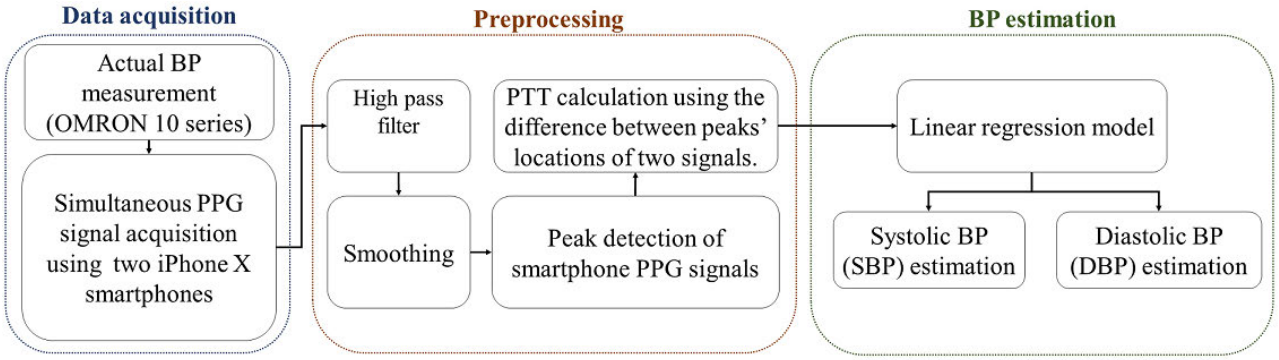

FIGURE 4. Flowchart of the BP estimation algorithm. After the data acquisition, the signals were preprocessed by passing through a high pass filter. The smoothing step eliminated undesired peaks before peak detection and the PTT calculation were performed. The estimated BP values were derived using a linear regression model.

a span of five data points was applied to the signals before peak detection was performed. Fig. 5 shows the raw PPG signals derived by the iOS application and the filtered signals from both left and right hands. As shown in Fig. 5b, this preprocessing approach made the signals overlap and enabled us to acquire the PTT between the peaks.

The peaks were detected by finding the local maximum values in the signals. We considered the fingertips of the index fingers of left and right hands as selected arterial sites. The PTT was directly measured between the maximum peak points of the two smartphone PPG signals gathered from the subject's index fingers within each cycle and derived from the time gap between the peaks' locations in the recorded PPG signals. An example of peak detection performed on two PPG signals, along with the defined PTT, is shown in Fig. 6.

Moreover, we performed the same procedure of filtering and peak detection for the NeXus PPG signals gathered from one test subject to compare the accuracy of capturing PTT values from the smartphone's camera, as described in Section II. Fig. 7 shows the filtered PPG signals (0 sec-14 sec) from both smartphones (see Fig. 7a) and the NeXus device (see Fig. 7b), and an example of the PTT for both signals (see Fig. 7c).

B. PTT AND BP ESTIMATION

PTT is a physiological parameter defined as the time difference of the pulse wave moving between different parts of an arterial site. Studies have been done to relate BP to PTT value. Different mathematical models, such as linear and non-linear models, have been introduced to estimate BP from PTT values. For this purpose, the arterial vessels have been modeled using a tube with the elasticity characteristic of the arterial walls [4].

PTT is mathematically defined as [4]:

$$PTT = l\sqrt{LC(P)}, \tag{1}$$

where l is the arterial length, and $L = \rho/A$ is a constant that represents the pressure difference in the arterial sites per the unit length, and is defined by the density of the blood (ρ) over the cross-section of the vessel (A). Here, C is a function of pressure P (blood pressure in the arterial site), which can be described as:

$$C(P) = \frac{A_m}{\pi P_1 \left[1 + \left(\frac{P-P_0}{P_1}\right)^2\right]}, \tag{2}$$

where A_m, P_0, and P_1 are the physical parameters derived specifically for each individual [52]. Thus, the BP estimation using the PTT should consider these individual-specific parameters and should be calculated separately for each person for accuracy. It is shown that these parameters are related to the individual's age, height, and other physiological parameters [4]. Considering these parameters and using equations (1) and (2), the relationship between BP and PTT can be

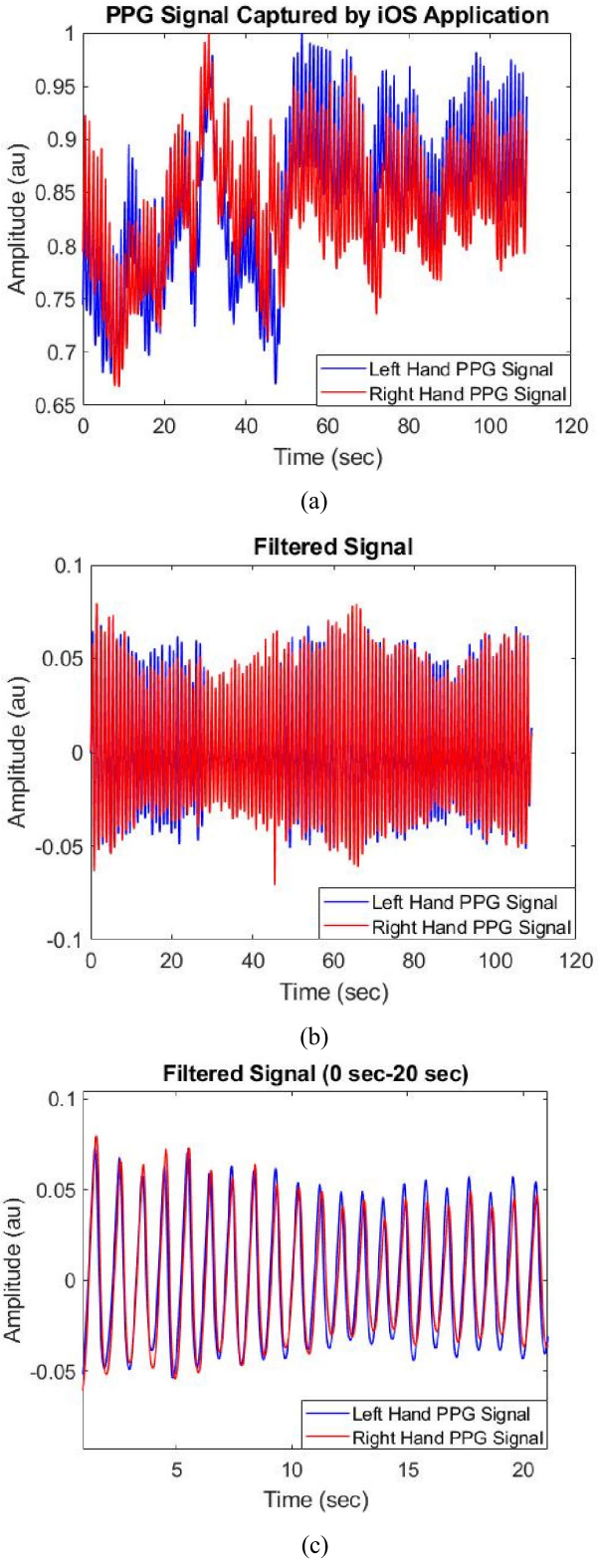

FIGURE 5. The raw PPG signals, and the preprocessed PPG signals. (a) The PPG signals captured by the smartphone application, and (b) the PPG signals of both hands after passing through a high pass filter and moving average filter. The red line is the PPG signal from the fingertip of the right hand, and the blue line is the PPG signal from the fingertip of the left hand, and (c) the first 20 seconds of (b) for a clear representation of the filtered signals.

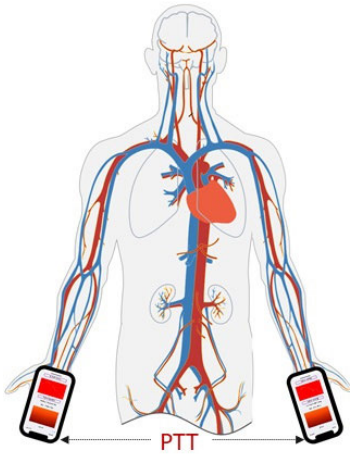

(a)

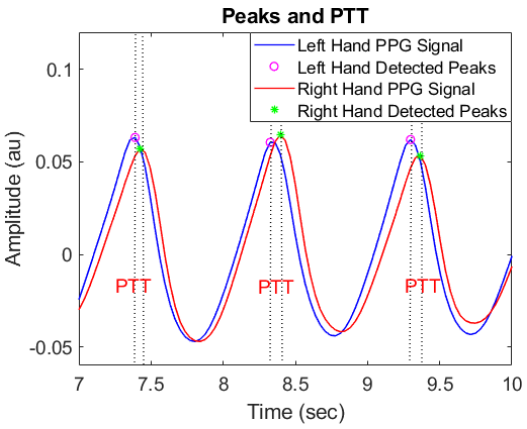

(b)

FIGURE 6. Schematic presentation of PTT. (a) The PTT is defined as the time difference between the two smartphone PPG signals, and (b) an example of peak detection performed on two filtered PPG signals, in which the PTT is defined as the time difference between the peaks' location in the two smartphone PPG signals.

modeled as [4], [53]:

$$BP = K_0 + \sqrt{K_1 + K_2 \frac{1}{PTT^2}}, \tag{3}$$

where K_0, K_1, and K_2 are the individual-specific parameters. This non-linear model can be simplified into one of the most well-known models presented as a linear relationship between the BP of a test subject and the inverse value of PTT using the following equation [4]:

$$BP = K_1 PTT^{-1} + K_2, \tag{4}$$

where K_is are the unknown individual-specific parameters of the BP estimation model.

The BP values are described by the systolic BP (SBP) and the diastolic BP (DBP) values. The PTT^{-1} is the inverse value of the average of all the PTT values during the 120-second measurement of each trial. Based on this model, the BP of the test subject should theoretically increase when the PTT^{-1} increases. Since the K_i parameters differ based upon the unique physiological structures of each individual [4], we derive the K_i values separately for each test subject.

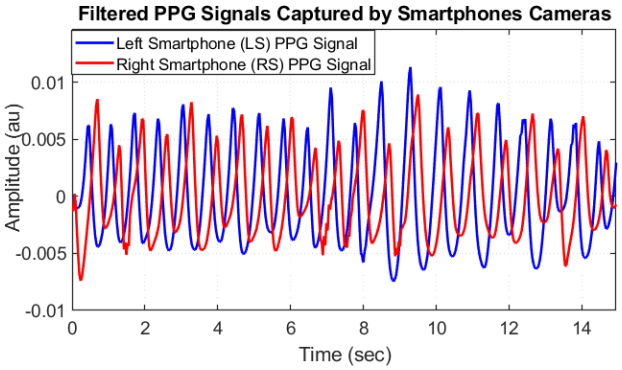

(a)

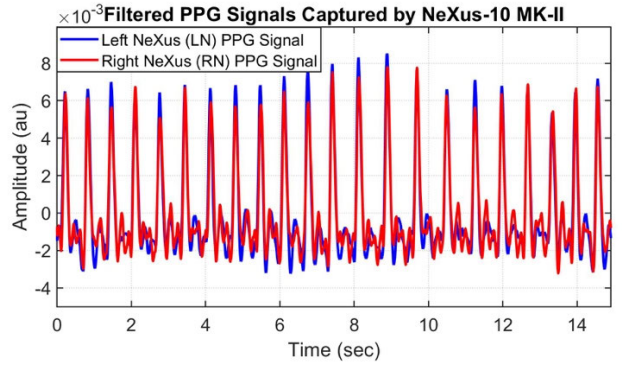

(b)

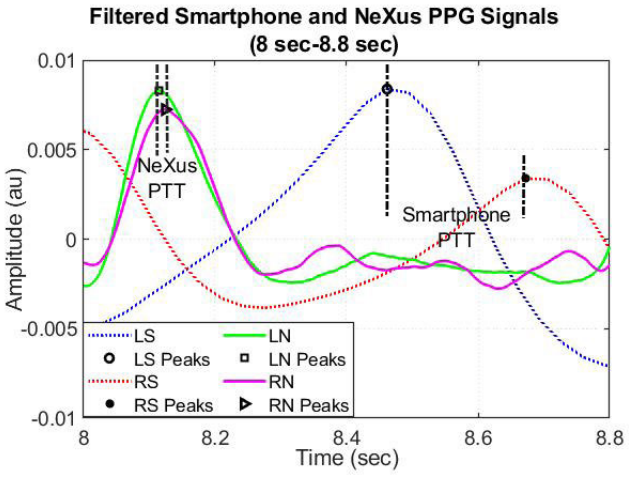

(c)

FIGURE 7. The PPG signals from the smartphones and the NeXus device measured for a test subject for the evaluation procedure. (a) The PPG signals (0 sec-14 sec) captured by the smartphone application from the left hand (LS, blue line) and the right hand (RS, red line). (b) The PPG signals (0 sec-14 sec) captured by the NeXus device from the left hand (LN, blue line) and the right hand (RN, red line). (c) Approximately 1 second of (a) and (b) for clear representation of the PTT for Nexus signals (solid green and solid magnet lines) and smartphone signals (dashed blue and dashed red lines).

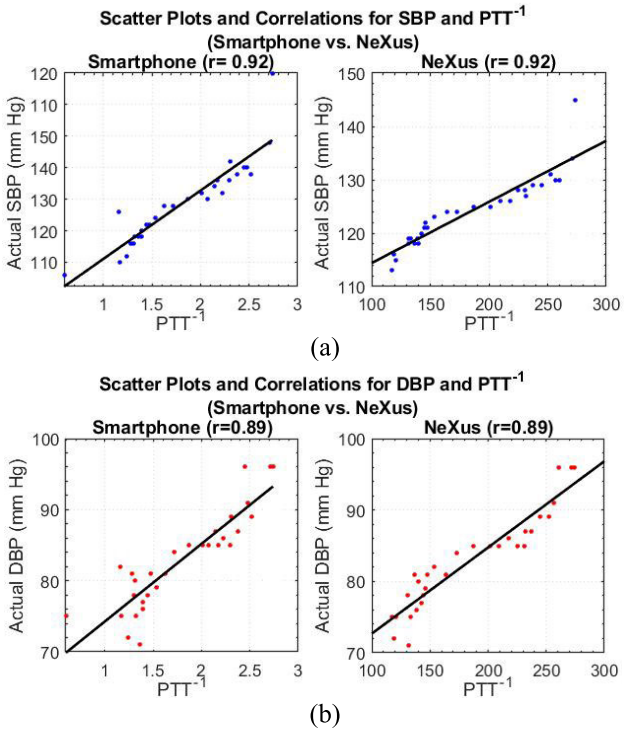

FIGURE 8. The scatter plots, correlations, and regression lines between the actual values of BP and the PTT^{-1} for smartphone signals and NeXus signals. The correlation coefficient (r) is presented in each plot. (a) The plots for SBP measurements and (b) the plot for the DBP measurements.

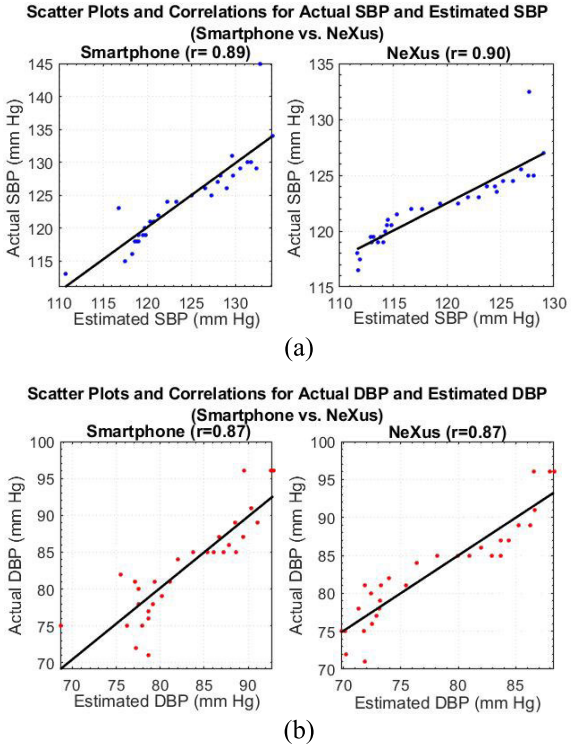

FIGURE 9. The scatter plots, correlations, and regression lines between the actual values of BP and the estimated values of BP for smartphone signals and NeXus signals. The correlation value (r) is presented in each plot. (a) The plots for SBP measurements and (b) for the DBP measurements.

To derive the K_i values, we used a linear regression model. Specifically, the linear regression model was applied to derive *1)* the K_i values of *SBP* ($K_{\mathrm{SBP},i}$) and *2)* the K_i values of *DBP* ($K_{\mathrm{DBP},i}$). We also derived the K_i parameters by training our linear regression model using a leave-one-out cross-validation algorithm. Hence, 29 trials of each subject were used to train the model and derive the K_i parameters. These K_i parameters were then used to estimate the *BP* of the remaining one trial as the test data compared with the actual BP value to evaluate our model. This process was repeated 30 times per subject, and the average values of all the 30 times are presented as the final results. The training and testing algorithms were applied distinctly for both SBP and DBP estimations separately.

IV. RESULTS

We gathered 180 trials of smartphone PPG signals and BP measurements from six subjects. As discussed in Section III, the PTT^{-1} values and the BP values are modeled to be correlated to each other by having a linear relationship.

Before conducting the actual measurements, we performed simultaneous PPG signals acquisition for one test subject using both smartphones' cameras and the NeXus device to evaluate the PTT estimation performance of our proposed system. As shown in Fig. 7, the PTT values from the NeXus PPG signals are slightly smaller compared to the smartphone signals (i.e. the PTT for NeXus $= 0.015$ and the PTT for smartphone $= 0.211$). We used the average values of all the captured PTT values from the signals of both hands to derive the PTT^{-1} value to estimate the BP.

We performed correlation analysis to evaluate our PTT^{-1} calculation from the smartphone PPG signals and NeXus signals with the actual BP measurements (i.e. SBP and DBP). Fig. 8a shows the scatter plots and correlations of our calculated PTT^{-1} values (i.e. smartphones value and NeXus value) with the actual SBP measurements obtained from the OMRON 10 series device. The scatter plots and correlations between the actual DBP measurements and the PTT^{-1} are shown in Fig. 8b. These results show that the actual BP (i.e. SBP and DBP) values are highly correlated to the PTT^{-1} values of smartphone and NeXus device (i.e. $r = 0.92$ for both smartphone and NeXus SBP measurements and $r = 0.89$ for both smartphone and NeXus DBP measurements; $p < 0.0005$). Fig. 9 shows the scatter plots and correlations between the estimated BP and actual BP of the test subject using the smartphones and NeXus device. As shown in Fig. 9a, the correlations between the estimated and actual SBP values for both NeXus and smartphone measurements are high and close to each other (i.e. $r = 0.90$ for NeXus and $r = 0.89$ for smartphone; $p < 0.0005$). The correlation coefficients for both NeXus and smartphones are equal for the estimated and actual DBP measurements (i.e. $r = 0.87$ for NeXus and $r = 0.87$ for smartphone; $p < 0.0005$).

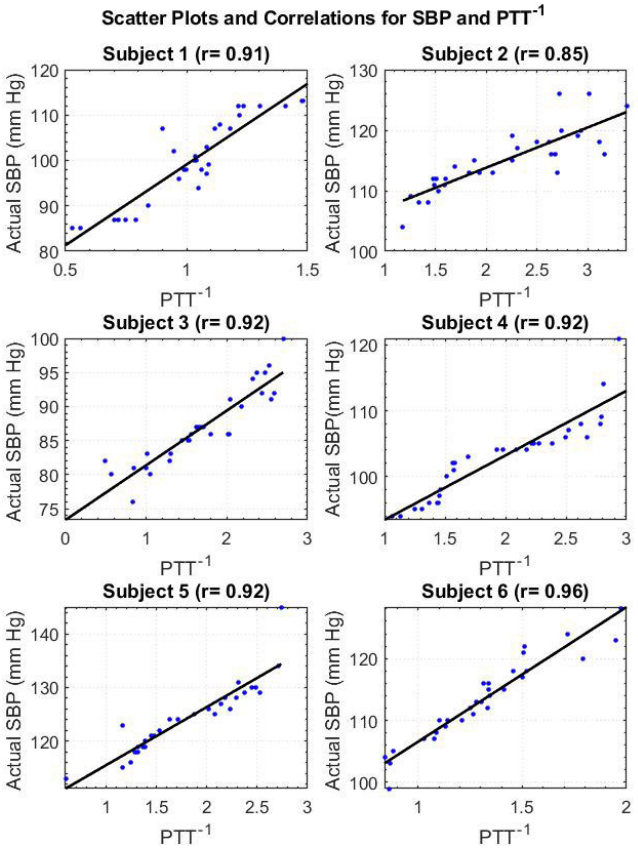

FIGURE 10. The scatter plots, correlations, and regression lines between the actual values of SBP and the PTT^{-1} for all the test subjects. The correlation coefficient (r) is presented in each plot.

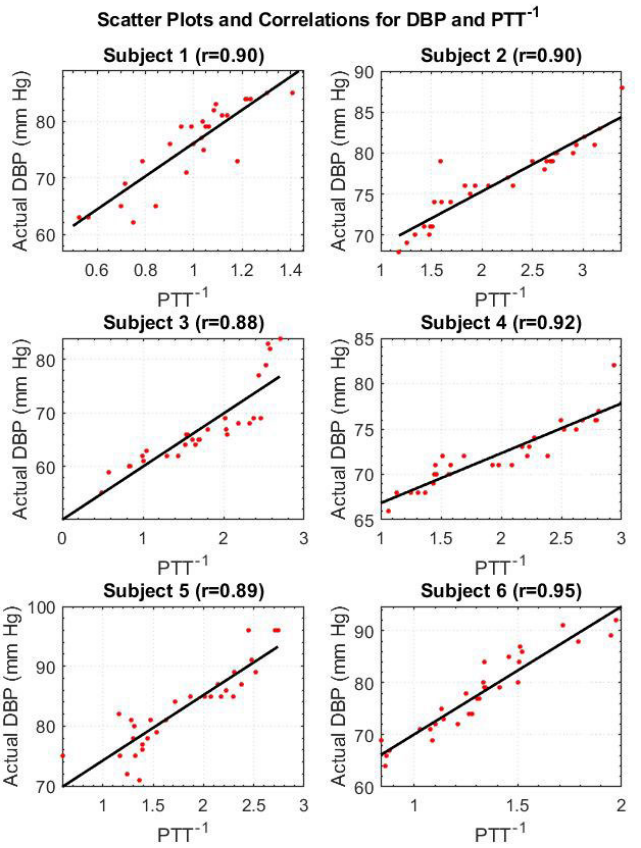

FIGURE 11. The scatter plots, correlations, and regression lines between the actual values of DBP and PTT^{-1} for all the test subjects. The correlation coefficient (r) is presented in each plot.

The mean absolute error (*MAE*), standard deviation of error (*SD*), and root-mean-square error (*RMSE*) values were calculated to evaluate the estimation accuracy of both measurements. That is, these statistical measurements are derived from the difference between the estimated values of the BP from the linear regression model and the actual BP values [54].

The *MAE*, *SD*, and *RMSE* for the NeXus were 1.81, 2.34, and, 2.82, respectively. For the smartphone, the *MAE*, *SD*, and *RMSE* were 1.74, 2.56, and 2.89, respectively. The results show that the smartphones' recordings agree with the NeXus device in terms of the discrepancy between the actual and estimated BP measurements. Therefore, the limited sampling frequency of the smartphone did not affect the accuracy of the measurement compared with the NeXus device.

Next, to evaluate our PTT^{-1} calculation from the smartphone PPG signals with the actual BP measurement (i.e. SBP and DBP) for all the subjects, we performed correlation analysis on all the test subjects. Fig. 10 shows the scatter plots and correlations for our calculated PTT^{-1} values and the actual SBP measurements obtained from the OMRON 10 series device. The scatter plots and correlations between the actual DBP measurement and the PTT^{-1} are shown in Fig. 11. As shown in Figs. 10 and 11, both BP measurements have significantly positive relationships with the PTT^{-1} (i.e. $r = 0.85$-0.96 for SBP and $r = 0.88$-0.95 for DBP; $p < 0.0005$) for all the test subjects.

Next, linear regression analysis was performed to estimate the $K_{\mathrm{SBP},i}$ and $K_{\mathrm{DBP},i}$ values for each test subject separately [23]. The estimated regression line was plotted for each subject in Figs. 10 and 11. The estimates of the K_1 and K_2 of the SBP and DBP for each subject from the linear regression model are presented in Table 1. Using the estimates of the K_1 and K_2 of the SBP and DBP, the *MAE*, *SD*, and *RMSE* values were calculated to evaluate the estimation accuracy of our model.

Tables 2 and 3 present the errors of SBP and DBP estimations for each subject, respectively. The maximum error was observed in the DBP estimation of Subject 1 with the *MAE*, *SD*, and *RMSE* of 3.28, 2.46, and, 4.02, respectively. According to the universal standard [55] between the Association for the Advancement of Medical Instrumentation (AAMI), the European Society of Hypertension (ESH), and the International Organization for Standardization (ISO) and the standard provided by Institute of Electrical and Electronics Engineers (IEEE) [56], an accurate BP estimation algorithm should have *MAE*

TABLE 1. Estimated K_i parameters of the SBP and DBP for each subject.

Subject	SBP Parameters		DBP Parameters	
	$K_{SBP,1}$	$K_{SBP,2}$	$K_{DBP,1}$	$K_{DBP,2}$
S1	36.57	62.64	28.84	47.28
S2	6.61	100.55	6.58	62.17
S3	8.12	73.14	9.99	49.90
S4	9.76	83.72	5.48	61.37
S5	11.27	103.72	11.37	62.33
S6	21.75	84.87	24.56	45.48

TABLE 2. Estimation error of the SBP analysis.

Subject	*MAE*	*SD*	*RMSE*
S1	3.28	2.46	4.02
S2	2.08	1.97	2.90
S3	1.87	1.65	2.42
S4	1.91	2.07	2.64
S5	1.74	2.56	2.90
S6	1.53	1.65	2.15

TABLE 3. Estimation error of the DBP analysis.

Subject	*MAE*	*SD*	*RMSE*
S1	2.78	2.08	3.53
S2	1.23	1.48	1.81
S3	2.98	2.49	3.72
S4	1.01	1.25	1.45
S5	2.54	2.13	3.25
S6	2.21	1.69	2.68

and *SD* values less than 5 mmHg and 8 mmHg, respectively. Our results presented in Tables 2 and 3 show that the maximum *MAE* and *SD* for SBP are 3.28 and 2.46, respectively. These values are 2.98 and 2.49 for the DBP measurements. Therefore, our results lie in an acceptable range of accuracy according to the mentioned standards.

We also examined the performance of our estimation model using the R-squared (R^2) value of the cross-validated linear regression model. This statistic indicates the percentage of the variation of the BP measurement accounted for the estimation model, which evaluates how well our model fits the data. The values of R^2 for both SBP and DBP are presented in Table 4. It was observed that more than 67% of the variance of BP measurements ($R^2 > 0.67$) was explained by the linear model for all the subject cases.

Next, we examined the relationships between the estimated BP values and the actual BP measurements using correlation analysis. It is expected that the estimated BP and the actual BP values have a positive linear relationship. Fig. 12 shows the scatter plots and correlations between the actual SBP values and the estimated SBP values. The scatter plots and correlations for the estimated DBP values and actual DBP values are shown in Fig. 13.

Strong relationships between the estimated and actual values of SBP and DBP (i.e. $r = 0.82$-0.95 for SBP and $r = 0.85$-0.94 for DBP, $p < 0.0005$) for all subjects may imply that our PPG acquisition method, PTT^{-1} calculation, and regression model have high accuracy in predicting the SBP and DBP.

TABLE 4. R-squared performance of the cross-validated linear regression model (SBP and DBP measurements).

Subject	R^2_{SBP}	R^2_{DBP}
S1	80.90%	78.84%
S2	67.18%	84.24%
S3	80.59%	72.64%
S4	80.99%	81.72%
S5	79.83%	76.18%
S6	89.44%	87.50%

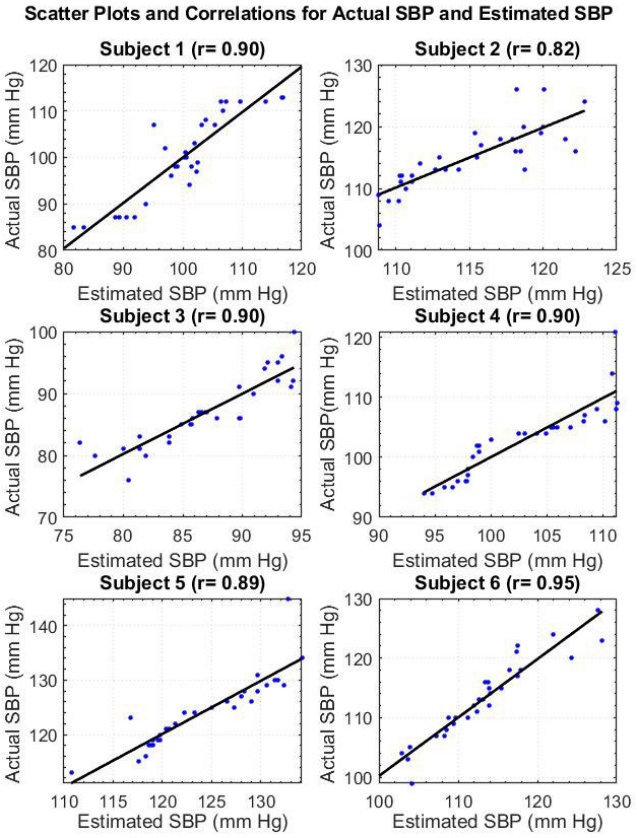

FIGURE 12. The scatter plots, correlations, and regression lines between the actual values of SBP and the estimated values of SBP for all test subjects. The correlation value (*r*) is presented in each plot.

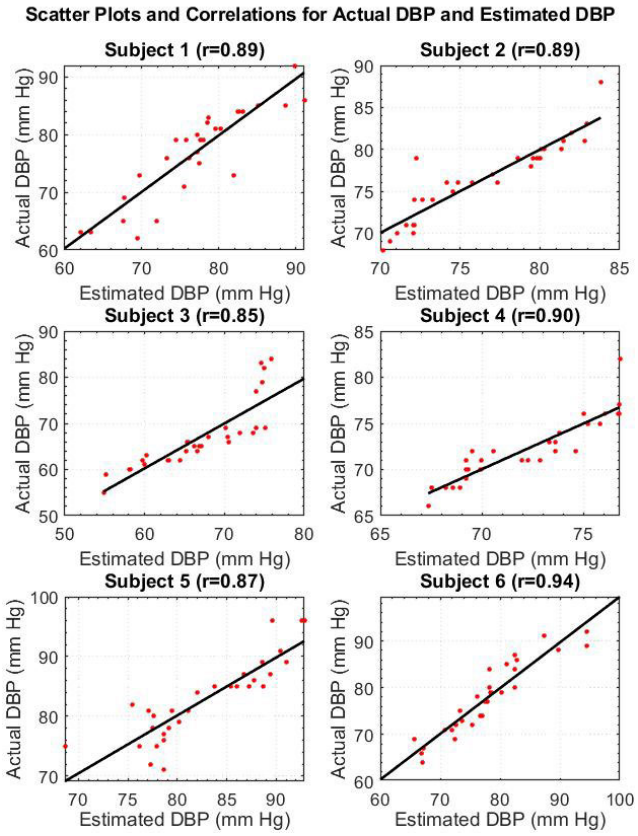

FIGURE 13. The scatter plots, correlations, and regression lines between the actual values of DBP and the estimated values of DBP for all test subjects. The correlation value (*r*) is presented in each plot.

V. DISCUSSION AND CONCLUSION

In this paper, we have proposed a cuff-less blood pressure estimation system by using only the smartphones' cameras. We have tested a new non-invasive portable BP monitoring system that uses our developed iOS app on two smartphones to estimate the continuous BP of six test subjects. The smartphones' cameras acquire two PPG signals from the index fingers of each participant. Environmental and physiological noise gathered during the experiment was minimized by applying filtration and smoothing on the PPG signals. Next, the peak detection technique was adopted to find the peaks. The BP was estimated from the time difference between the peaks of the PPG signals. This time difference is known as PTT, and the BP can be estimated using the PTT value.

Previous studies mainly focus on deriving the PTT from the time difference between the ECG signal and the PPG signal. It is also shown that PTT can be defined by the time difference between the blood pressure wave reaching two different arterial sites, the fingertip and the foot. However, the possibility of deriving PTT from the index fingers of two hands has not been evaluated for BP estimation. Recently, smartphones have emerged as useful in health care monitoring, although the possibility of deriving PTT from two different arterial sites using only smartphones' cameras has not been studied. Therefore, in this paper, we focused on proposing a BP estimation method which 1) uses the PTT from the index fingers of both hands and 2) adopts smartphone PPG signals for the PTT measurement.

Here, we used two smartphones to acquire the PPG signals from the fingertips of the left and right hands to evaluate the accuracy of the PTT and BP estimations, using two different arterial sites. We evaluated the performance of the smartphone in capturing PTT to provide accurate results by measuring smartphone PPG signals simultaneously with the reference PPG signals obtained by NeXus-10 MK II. The correlation coefficients between the PTT^{-1} values and the SBP and the DBP were identical for the NeXus and smartphones (i.e. $r = 0.92$ for SBP and $r = 0.89$ for DBP; $p < 0.0005$). Moreover, the correlations between the estimated and actual BP values from the smartphones were close to those derived from the NeXus device. Therefore, the limited sampling frequency of the smartphone results in allowable discrepancy in estimating the BP values.

Recently, advanced smartphones have been equipped with dual or triple cameras. As future work, the authors plan to use only one smartphone to acquire the PPG signals from the subjects' index fingers. In other words, the proposed method could be used in future using only one smartphone with no additional devices if we could overcome the limitation of using both cameras (i.e. front and rear cameras) of the smartphones simultaneously.

To estimate the BP from the PTT, a well-known mathematical model which relates the BP to the PTT was adopted. This mathematical model shows that the BP and PTT values have a linear relationship using individual-specific parameters (K_i). We used a linear regression model to acquire these parameters for each subject separately. Specifically, the K_i parameters were derived once for the SBP estimation and once for the DBP estimation of all the test subjects.

These parameters have been tested, and the accuracy of our estimation has been evaluated, by comparing the predicted BP values with the actual BP. The actual BP was derived using the OMRON 10 series digital BP monitoring device. The correlation analysis between the actual BP and the estimated BP have shown that the estimated SBP values of all the subjects are highly correlated with the actual SBP values (i.e.$r = 0.82$-0.95, $p < 0.0005$). The correlation coefficients for our estimated DBP also showed a strong relationship with the actual DBP values (i.e. $r = 0.85$-0.94, $p < 0.0005$). The *MAE* for both the SBP and DBP is less than 5mm Hg. The maximum deviation of error (i.e. the *SD*) was 2.46 for SBP and 2.49 for DBP estimation. These results agreed with the IEEE standard for the cuff-less BP estimation methods. Moreover, we performed an R^2 value of the cross-validation, which shows an accurate fitting for SBP and DBP ($R^2 > 67\%$).

Although to the authors' knowledge there is not any study using smartphone PPG signals from both hands to acquire PTT, we evaluated the performance of our smartphone-based BP system with two other studies. Table 5 shows a comparison of our model with previous studies. As shown in Table 5, the average error between the actual and estimated

TABLE 5. Comparison of the proposed smartphone-based BP method with previous studies.

Study	Average MAE	Average SD	r
Our system	2.10	1.96	0.90
[57]	13.99	-	-
[53]	7.47	11.08	0.80

BP values is significantly less in our study compared to the others, while maintaining the accuracy in terms of correlation parameter ($r = 0.90$). The results of this study compared with previous studies indicates the possibility of using smartphone PPG signals acquired from the fingertips of both hands. Since smartphone PPG signals are easily affected with MNA, an MNA detection algorithm that enables detecting and removing MNA from both smartphone PPG signals in a synchronized way could be adopted in future studies to increase the accuracy of the measurements.

ACKNOWLEDGMENT

(Fatemehsadat Tabei and Jon Michael Gresham contributed equally to this work.)

REFERENCES

[1] (2019). *Centers For Disease Control And Prevention (CDC)*. High Blood Pressure. [Online]. Available: [Online]. Available: https://www.cdc.gov/bloodpressure/index.htm
[2] (2019). *World Health Organization (WHO)*. [Online]. Available: [Online]. Available: https://www.who.int/news-room/fact-sheets/detail/hypertension
[3] *American Heart Association, Center for Health Metrics and Evaluation. Four Principles to Help Control the High Cost of High Blood Pressure*. Accessed: Nov. 10, 2019. [Online]. Available: https://healthmetrics.heart.org/four-principles-to-help-control-the-high-cost-of-high-blood-pressure/
[4] R. Mukkamala, J.-O. Hahn, O. T. Inan, L. K. Mestha, C.-S. Kim, H. Toreyin, and S. Kyal, "Toward ubiquitous blood pressure monitoring via pulse transit time: Theory and practice," *IEEE Trans. Biomed. Eng.*, vol. 62, no. 8, pp. 1879–1901, Aug. 2015.
[5] D. Perloff, C. Grim, J. Flack, E. D. Frohlich, M. Hill, M. McDonald, and B. Z. Morgenstern, "Human blood pressure determination by sphygmomanometry," *Circulation*, vol. 88, no. 5, pp. 2460–2470, 1993.
[6] B. S. Alpert, D. Quinn, and D. Gallick, "Oscillometric blood pressure: A review for clinicians," *J. Amer. Soc. Hypertension*, vol. 8, no. 12, pp. 930–938, Dec. 2014.
[7] G. Drzewiecki, R. Hood, and H. Apple, "Theory of the oscillometric maximum and the systolic and diastolic detection ratios," *Ann. Biomed. Eng.*, vol. 22, no. 1, pp. 88–96, Jan. 1994.
[8] G. M. Drzewiecki, J. Melbin, and A. Noordergraaf, "Deformational forces in arterial tonometry," in *Proc. IEEE/Eng. Med. Biol. Soc. Annu. Conf.*, 1984, pp. 642–645.
[9] J. S. Eckerle, "Tonometry, arterial," in *Encyclopedia of Medical Devices and Instrumentation*, J. G. Webster, Ed. 2006, doi: 10.1002/0471732877.emd25.
[10] A. Stojanova, S. Koceski, and N. Koceska, "Continuous blood pressure monitoring as a basis for ambient assisted living (AAL)–review of methodologies and devices," *J. Med. Syst.*, vol. 43, no. 2, p. 24, Jan. 2019.
[11] B. Imholz, "Fifteen years experience with finger arterial pressure monitoring: Assessment of the technology," *Cardiovascular Res.*, vol. 38, no. 3, pp. 605–616, Jun. 1998.
[12] D. M. Bard, J. I. Joseph, and N. van Helmond, "Cuff-less methods for blood pressure telemonitoring," *Frontiers Cardiovascular Med.*, vol. 6, p. 40, Apr. 2019.
[13] R. Agarwal and R. P. Light, "The effect of measuring ambulatory blood pressure on nighttime sleep and daytime activity—Implications for dipping," *Clin. J. Amer. Soc. Nephrol.*, vol. 5, no. 2, pp. 281–285, 2010.
[14] G. Parati, E. Dolan, R. J. Mcmanus, and S. Omboni, "Home blood pressure telemonitoring in the 21st century," *J. Clin. Hypertension*, vol. 20, no. 7, pp. 1128–1132, Jul. 2018.
[15] Y.-Z. Yoon, J. M. Kang, Y. Kwon, S. Park, S. Noh, Y. Kim, J. Park, and S. W. Hwang, "Cuff-less blood pressure estimation using pulse waveform analysis and pulse arrival time," *IEEE J. Biomed. Health Inform.*, vol. 22, no. 4, pp. 1068–1074, Jul. 2018.
[16] Y. Chen, C. Wen, G. Tao, M. Bi, and G. Li, "Continuous and noninvasive blood pressure measurement: A novel modeling methodology of the relationship between blood pressure and pulse wave velocity," *Ann. Biomed. Eng.*, vol. 37, no. 11, pp. 2222–2233, Nov. 2009.
[17] F. S. Cattivelli and H. Garudadri, "Noninvasive cuffless estimation of blood pressure from pulse arrival time and heart rate with adaptive calibration," in *Proc. 6th Int. Workshop Wearable Implant. Body Sensor Netw.*, Jun. 2009, pp. 114–119.
[18] J. Muehlsteff, X. A. Aubert, and G. Morren, "Continuous cuff-less blood pressure monitoring based on the pulse arrival time approach: The impact of posture," in *Proc. 30th Annu. Int. Conf. IEEE Eng. Med. Biol. Soc.*, Aug. 2008, pp. 1691–1694.
[19] S. S. Thomas, V. Nathan, C. Zong, E. Akinbola, A. Lourdes P. Aroul, L. Philipose, K. Soundarapandian, X. Shi, and R. Jafari, "BioWatch—A wrist watch based signal acquisition system for physiological signals including blood pressure," in *Proc. 36th Annu. Int. Conf. IEEE Eng. Med. Biol. Soc.*, Aug. 2014, pp. 2286–2289.
[20] A. M. Zakrzewski and B. W. Anthony, "Arterial blood pressure estimation using ultrasound: Clinical results on healthy volunteers and a medicated hypertensive volunteer," in *Proc. 39th Annu. Int. Conf. IEEE Eng. Med. Biol. Soc. (EMBC)*, Jul. 2017, pp. 2154–2157.
[21] D. Zheng and A. Murray, "Non-invasive quantification of peripheral arterial volume distensibility and its non-linear relationship with arterial pressure," *J. Biomech*, vol. 42, no. 8, pp. 1032–1037, May 2009.
[22] W.-H. Lin, H. Wang, O. W. Samuel, and G. Li, "Using a new PPG indicator to increase the accuracy of PTT-based continuous cuffless blood pressure estimation," in *Proc. 39th Annu. Int. Conf. IEEE Eng. Med. Biol. Soc. (EMBC)*, Jul. 2017, pp. 738–741.
[23] R. Wang, W. Jia, Z.-H. Mao, R. J. Sclabassi, and M. Sun, "Cuff-free blood pressure estimation using pulse transit time and heart rate," in *Proc. 12th Int. Conf. Signal Process. (ICSP)*, Oct. 2014, pp. 115–118.
[24] S. Sun, R. Bezemer, X. Long, J. Muehlsteff, and R. M. Aarts, "Systolic blood pressure estimation using PPG and ECG during physical exercise," *Physiol. Meas.*, vol. 37, no. 12, pp. 2154–2169, Dec. 2016.
[25] D. B. Mccombie, A. T. Reisner, and H. H. Asada, "Adaptive blood pressure estimation from wearable PPG sensors using peripheral artery pulse wave velocity measurements and multi-channel blind identification of local arterial dynamics," in *Proc. Int. Conf. IEEE Eng. Med. Biol. Soc.*, Aug. 2006, pp. 3521–3524.
[26] M. K. B. A. Hassan, M. Y. Mashor, N. F. Mohd Nasir, and S. Mohamed, *Measuring of Systolic Blood Pressure Based On Heart Rate*. Berlin, Germany: Springer, 2008, pp. 595–598.
[27] E. Nemati, M. Deen, and T. Mondal, "A wireless wearable ECG sensor for long-term applications," *IEEE Commun. Mag.*, vol. 50, no. 1, pp. 36–43, Jan. 2012.
[28] C. Poon and Y. Zhang, "Cuff-less and noninvasive measurements of arterial blood pressure by pulse transit time," in *Proc. IEEE Eng. Med. Biol. 27th Annu. Conf.*, 2005, pp. 5877–5880.
[29] M. Kachuee, M. M. Kiani, H. Mohammadzade, and M. Shabany, "Cuffless blood pressure estimation algorithms for continuous health-care monitoring," *IEEE Trans. Biomed. Eng.*, vol. 64, no. 4, pp. 859–869, Apr. 2017.
[30] N. Kumar, A. Agrawal, and S. Deb, "Cuffless BP measurement using a correlation study of pulse transient time and heart rate," in *Proc. Int. Conf. Adv. Comput., Commun. Inform. (ICACCI)*, Sep. 2014, pp. 1538–1541.
[31] S.-Y. Ye, G.-R. Kim, D.-K. Jung, S. W. Baik, and G. R. Jeon, "Estimation of systolic and diastolic pressure using the pulse transit time," *World Acad. Sci. Eng. Technol.*, vol. 67, pp. 726–731, Jul. 2010.
[32] S. Ghosh, A. Banerjee, N. Ray, P. W. Wood, P. Boulanger, and R. Padwal, "Continuous blood pressure prediction from pulse transit time using ECG and PPG signals," in *Proc. IEEE Healthcare Innov. Point-Of-Care Technol. Conf. (HI-POCT)*, Nov. 2016, pp. 188–191.
[33] A.-G. Pielmuç, M. Pflugradt, T. Tigges, M. Klum, A. Feldheiser, O. Hunsicker, and R. Orglmeister, "Novel computation of pulse transit time from multi-channel PPG signals by wavelet transform," *Current Directions Biomed. Eng.*, vol. 2, no. 1, pp. 209–213, 2016.
[34] Omron. (2019). *HeartGuide Wearable Blood Pressure Monitor*. [Online]. Available: https://omronhealthcare.com/products/heartguide-wearable-blood-pressure-monitor-bp8000m/

[35] BodiMetrics. *BodiMetricsTM Wrist Blood Pressure Monitor*. Accessed: Nov. 10, 2019. [Online]. Available: https://bodimetrics.com/product/wrist-blood-pressure-monitor/
[36] Qardio. *QardioArm*. [Online]. Available: https://store.getqardio.com/products/qardioarm
[37] C. Holz and E. J. Wang, "Glabella: Continuously sensing blood pressure behavior using an unobtrusive wearable device," *ACM Interact., Mobile, Wearable Ubiquitous Technol.*, vol. 1, no. 3, pp. 1–23, 2017.
[38] R. Lazazzera, Y. Belhaj, and G. Carrault, "A new wearable device for blood pressure estimation using photoplethysmogram," *Sensors*, vol. 19, no. 11, p. 2557, Jun. 2019.
[39] J. W. Chong, C. H. Cho, F. Tabei, D. Le-Anh, N. Esa, D. D. Mcmanus, and K. H. Chon, "Motion and noise artifact-resilient atrial fibrillation detection using a smartphone," *IEEE J. Emerg. Sel. Topics Circuits Syst.*, vol. 8, no. 2, pp. 230–239, Jun. 2018.
[40] I. Tayfur, and M. A. Afacan, "Reliability of smartphone measurements of vital parameters: A prospective study using a reference method," *Amer. J. Emergency Med.*, vol. 37, no. 8, pp. 1527–1530, Aug. 2019.
[41] S. S. Mousavi, M. Firouzmand, M. Charmi, M. Hemmati, M. Moghadam, and Y. Ghorbani, "Blood pressure estimation from appropriate and inappropriate PPG signals using A whole-based method," *Biomed. Signal Process. Control*, vol. 47, pp. 196–206, Jan. 2019.
[42] V. Chandrasekaran, R. Dantu, S. Jonnada, S. Thiyagaraja, and K. P. Subbu, "Cuffless differential blood pressure estimation using smart phones," *IEEE Trans. Biomed. Eng.*, vol. 60, no. 4, pp. 1080–1089, Apr. 2013.
[43] F. Tabei, R. Zaman, K. H. Foysal, R. Kumar, Y. Kim, and J. W. Chong, "A novel diversity method for smartphone camera-based heart rhythm signals in the presence of motion and noise artifacts," *PLoS ONE*, vol. 14, no. 6, Jun. 2019, Art. no. e0218248.
[44] F. Tabei, R. Kumar, T. N. Phan, D. D. Mcmanus, and J. W. Chong, "A novel personalized motion and noise artifact (MNA) detection method for smartphone photoplethysmograph (PPG) signals," *IEEE Access*, vol. 6, pp. 60498–60512, 2018.
[45] H. Liu, K. Ivanov, Y. Wang, and L. Wang, "Toward a smartphone application for estimation of pulse transit time," *Sensors*, vol. 15, no. 10, pp. 27303–27321, Oct. 2015.
[46] (Sep. 10, 2019). *iCare Health Monitor*. Available:. [Online]. Available: http://www.icarefit.com
[47] M. Elgendi, R. Fletcher, Y. Liang, N. Howard, N. H. Lovell, D. Abbott, K. Lim, and R. Ward, "The use of photoplethysmography for assessing hypertension," *npj Digit. Med.*, vol. 2, no. 1, p. 60, Jun. 2019.
[48] E. J. Wang, "Seismo: Blood pressure monitoring using built-in smartphone accelerometer and camera," in *Proc. CHI Conf. Hum. Factors Comput. Syst.*, vol. 2018, p. 425.
[49] Apple. (2019). *iPhone X–Technical Specifications*. [Online]. Available: https://support.apple.com/kb/sp770?locale=en_US
[50] OMRON. (2015). *10 series Blood Pressure Monitor,Model BP786N,Instruction Manual [nstruction Manual]*. [Online]. Available: https://omronhealthcare.com/wp-content/uploads/BP786N-IM_EN.pdf
[51] Mind Media. (2019). *NeXus-10 MKII*. Accessed: Nov. 10, 2019. [Online]. Available: https://www.mindmedia.com/en/products/nexus-10-mkii/
[52] G. Langewouters, K. Wesseling, and W. Goedhard, "The static elastic properties of 45 human thoracic and 20 abdominal aortas in vitro and the parameters of a new model," *J. Biomech.*, vol. 17, no. 6, pp. 425–435, Jan. 1984.
[53] A. E. Dastjerdi, M. Kachuee, and M. Shabany, "Non-invasive blood pressure estimation using phonocardiogram," in *Proc. IEEE Int. Symp. Circuits Syst. (ISCAS)*, May 2017, pp. 1–4.
[54] I. Sharifi, S. Goudarzi, and M. B. Khodabakhshi, "A novel dynamical approach in continuous cuffless blood pressure estimation based on ECG and PPG signals," *Artif. Intell. Med.*, vol. 97, pp. 143–151, Jun. 2019.
[55] G. S. Stergiou, "A universal standard for the validation of blood pressure measuring devices," *Hypertension*, vol. 71, no. 3, pp. 368–374, 2018.
[56] *IEEE Standard for Wearable Cuffless Blood Pressure Measuring Devices*, IEEE Standard 1708-2014, 2014, pp. 1–38.
[57] A. Dias Junior, S. Murali, F. Rincon, and D. Atienza, "Methods for reliable estimation of pulse transit time and blood pressure variations using smartphone sensors," *Microprocessors Microsyst.*, vol. 46, pp. 84–95, Oct. 2016.

FATEMEHSADAT TABEI received the B.S. and M.S. degrees in electrical engineering from Shiraz University, Shiraz, Iran. She is currently pursuing the Ph.D. degree with Texas Tech University, USA. Her current research interests include biomedical signal processing, biomedical image processing, and machine learning.

JON MICHAEL GRESHAM received the B.S. degree in computer engineering from Texas Tech University, USA, in 2014, where he is currently pursuing the M.S. degree in electrical and computer engineering. His current research interests include biomedical signal processing, non-invasive physiological monitoring, RF system-on-a-chip design, medical electronics, and biosensors.

BEHNAM ASKARIAN received the B.S. and M.S. degrees in electrical engineering from Shiraz University, Shiraz, Iran. He is currently pursuing the Ph.D. degree with Texas Tech University, USA. His current research interests include biomedical image processing, machine learning, and monitoring of health and disease using smartphones.

KWANGHEE JUNG received the Ph.D. degree in quantitative psychology from McGill University, in 2012. He was a Postdoctoral Fellow with The University of British Columbia, from 2011 to 2012, an Assistant Professor with The University of Texas Health Science Center at Houston, from 2013 to 2016, and a Research Scientist with ACT, Inc., from 2016 to 2017. Since 2017, he has been an Assistant Professor with Texas Tech University. His research has focused on the development and applications of quantitative methods, measurement, and advanced modeling methodologies to diverse issues and topics in brain imaging data analysis, bio-medical and patient-reported outcomes research, mental health and disorders, and human development and education.

JO WOON CHONG received the B.S., M.S., and Ph.D. degrees in electrical engineering from the Korea Advanced Institute of Science and Technology, Daejeon, South Korea, in 2002, 2004, and 2009, respectively. From 2010 to 2012, he was a Postdoctoral Fellow with the Massachusetts Institute of Technology (MIT). He was a Research Assistant Professor with the Worcester Polytechnic Institute, USA, from 2012 to 2016. Since 2016, he has been an Assistant Professor with Texas Tech University, USA. His current research interests include biomedical signal processing, non-invasive physiological monitoring, sensors and wireless communication for medical care, machine learning techniques for healthcare data, and home monitoring of health and disease.